Modeling Remote-Sensing Reflectance and Retrieving Chlorophyll-a Concentration in Extremely Turbid Case-2 Waters (Lake Taihu, China)

Yunlin Zhang, Mingliang Liu, Boqiang Qin, Hendrik Jan van der Woerd, Junsheng Li, and Yunliang Li

***Abstract*—Accurate assessment of concentration of chlorophyll a (Chl*a*) and correct identification of algal blooms by remote sensing have previously been a great challenge in the optically complex Case-2 waters. In this paper, we used a large biooptical data set to model the remote-sensing reflectance in an extremely turbid and biologically productive Lake Taihu in China. The conceptual three-band model $[R_{\mathrm{rs}}^{-1}(\lambda_1) - R_{\mathrm{rs}}^{-1}(\lambda_2)] \times R_{\mathrm{rs}}(\lambda_3)$ (where R_{rs} represents remote-sensing reflectance just above the water surface) to retrieve Chl*a* concentration was calibrated and validated, and a detailed assessment of its accuracy was obtained. Water samples were collected for four seasons from 2006 to 2007 at 50 sites, covering different ecosystem types, and contained three very variable optically active substances (tripton 7.9–281.7 mg $\cdot$ L^{-1}, Chl*a* 4.0–448.9 $\mu\mathrm{g} \cdot \mathrm{L}^{-1}$, and chromophoric dissolved organic matter $[a_{\mathrm{CDOM}}(440)]$ 0.27–2.36 m^{-1}). Secchi disk transparency ranged from 8 to 85 cm. The retrieval accuracies (r^2) of the optimal three-band model and the related band-ratio method were 0.94 and 0.92, while the root mean-square errors (RMSE) and relative errors (RE) were 15.1 $\mu\mathrm{g} \cdot \mathrm{L}^{-1}$ (37.3% accounting for the mean value) and 18.0 $\mu\mathrm{g} \cdot \mathrm{L}^{-1}$, and 44.4% and 60.2%, respectively. Applications of the three-band model using MERIS central bands $[R_{\mathrm{rs}}^{-1}(681) - R_{\mathrm{rs}}^{-1}(709)] \times R_{\mathrm{rs}}(754)$ also allowed accurate estimation of Chl*a,* with r^2, RMSE, and RE of 0.92, 17.0 $\mu\mathrm{g} \cdot \mathrm{L}^{-1}$, and 48.1%, respectively. The establishment of a simple and robust biooptical model with high retrieval accuracy and known error budgets will help the rapid, accurate, and real-time assessment of algal blooms using *in situ* and satellite remote-sensing techniques.**

***Index Terms*—Absorption coefficient, chlorophyll a (Chl*a*), error budgets, Lake Taihu, remote-sensing reflectance.**

I. Introduction

In THE LAST 20 years, increased nutrient loadings, driven by industrial development, human-population growth, and changes in land use, have resulted in eutrophication and increased phytoplankton concentrations in Lake Taihu in China [1]. In recent summers, the accumulation of surface blooms of the cyanobacteria *Microcystis spp.* has impeded normal operation of drinking-water plants for the large cities of Wuxi and Wujing, and from May to October, particularly high cyanobacterial concentrations have been recorded in Meiliang Bay and Zhushan Bay within the lake. In particular, in early June in 2007, a cyanobacterial bloom in Gonghu Bay polluted the biggest drinking-water plant in Wuxi City, interrupting water supply in Wuxi City for several days. Furthermore, the cyanobacterial blooms in Lake Taihu pose additional potential health risks, due to the toxic *Microcystis spp.*, particularly in summer [2]. Exposure to toxic *Microcystis spp.* could lead to liver failure in wild animals, livestock, and aquatic life, as well as human illnesses and mortality. Some reports suggest that the incidence of human primary liver cancer in the eastern region of China is related to the presence of microcystins found in drinking water [3], [4].

Conventional chlorophyll-a (Chl*a*) monitoring programs are limited in their effectiveness in Lake Taihu, because they only provide spatial distribution data of Chl*a* concentration along their routes during fixed cruises. The restricted temporal and spatial aspects of such conventional ship-based water-sampling programs are not adequate to report changes in phytoplankton biomass. This is particularly problematic during bloom conditions when the variability in phytoplankton density is particularly high, with accumulations happening in time periods as brief as several hours or within a single day, and when there is frequent disturbance due to wind waves. The serious 2007 contamination of the water supply to Wuxi City was not detected because the algal-bloom accumulation and deposition were not recognized due to the low frequency and small area of conventional sampling.

In order to mitigate the impacts of algal blooms and issue warnings to drinking-water plants in Lake Taihu, it is therefore essential to detect, monitor, and forecast the development and movement of blooms using more detailed and effective techniques. In some coastal and lake waters, the use of airborne and satellite remote sensing has demonstrated to provide more reliable temporal–spatial information about water quality and the extent of the cyanobacterial blooms than does conventional monitoring [5]–[9]. Thus, this approach was adopted for Lake Taihu.

Lake Taihu is a large eutrophic shallow lake with high spatial heterogeneity; different ecosystem types (algal-dominated, macrophyte-dominated, and transition regions); complicated dynamics of phytoplankton, particulate matter, and chromophoric dissolved organic matter (CDOM); and variable

Manuscript received July 1, 2008; revised September 12, 2008 and October 29, 2008. This work was supported in part by the Knowledge Innovation Project of the Chinese Academy of Sciences under Grants KZCX1-YW-14-2 and KZCX2-YW-419 and in part by the National Natural Science Foundation of China under Grant 40730529.

Y. Zhang, M. Liu, B. Qin, and Y. Li are with Taihu Lake Laboratory Ecosystem Research Station, State Key Laboratory of Lake Science and Environment, Nanjing Institute of Geography and Limnology, Chinese Academy of Sciences, Nanjing 210008, China (e-mail: ylzhang@niglas.ac.cn).

H. J. van der Woerd is with the Institute for Environmental Studies, Vrije Universiteit, 1081 HV Amsterdam, The Netherlands.

J. Li is with the Earth Observation and Digital Earth Science Center, Chinese Academy of Sciences, Beijing 100080, China.

Digital Object Identifier 10.1109/TGRS.2008.2011892

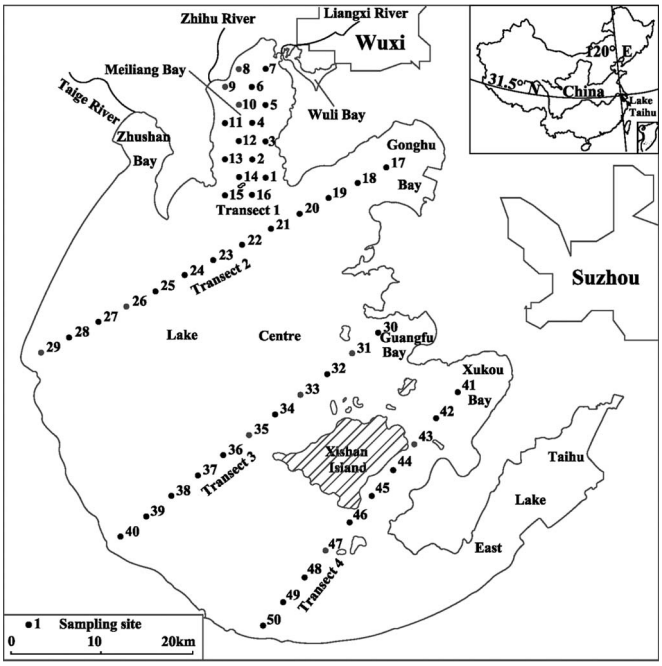

Fig. 1. Distribution of transects and sampling sites.

biooptical properties [10]–[12]. Remote sensing is a potentially powerful tool for studying phytoplankton dynamics and managing water quality in the Lake Taihu by virtue of its ability to resolve steep spatial gradients and temporal variability in optically significant constituents. However, despite this potential, such an approach has not been widely used, and the temporal–spatial variations of biooptical properties and the concentrations of three optically active substances (tripton, phytoplankton, and CDOM) in Lake Taihu remain poorly characterized. As a result, most studies have focused on the collection of data for optically active substances based on the *in situ* measurement of the remote-sensing reflectance [13], [14]. To address this need, the aims of this paper are as follows: 1) compare the variations of the concentrations and spectral absorption coefficients of three optically active substances for four different seasons; 2) model the remote-sensing reflectance and discuss its spectral characteristics; 3) optimize a three-band model to estimate Chl*a* concentration; and 4) characterize the error budget of the retrieval model.

II. Materials and Methods

A. Study Site and Sampling Schedule

Optical measurements were made and water samples were taken at 50 sites in different regions of the lake: transect 1 (sites 1–16) followed a semicircular route around Meiliang Bay in the north, transect 2 (sites 17–29) originated in Gonghu Bay and extended southwest across the lake center, transect 3 (sites 30–40) originated in Guanghu Bay and extended southwest across the lake center, and transect 4 (sites 41–50) originated in Xukou Bay and extended southwest across the lake, passing south of Xishan Island (Fig. 1). Measurements and water samples were taken on four seasonal cruises: winter (January 7–9, 2006), spring (April 25–27, 2007), summer (July 28–August 1, 2006), and autumn (October 12–15, 2006).

In order to validate the three-band model and band-ratio method used to estimate Chl*a* concentration, an independent data set ($32 \times 2 = 64$ samplings) was obtained from two sampling cruises in May (17–19) and October (16–18) in 2005. The sample sites in these investigations were basically evenly distributed over the Lake Taihu [15].

B. Sample Preparation

Samples for Chl*a* were filtered on Whatman GF/C fiberglass filters. The Chl*a* and phaeophytin *a* (P*a*) were extracted with ethanol (90%) at 80 °C and analyzed spectrophotometrically at 750 and 665 nm with correction for P*a*.

To obtain total suspended matter (TSM), water samples were filtered through precombusted Whatman GF/C fiberglass filters (450 °C for 4 h) to remove suspended organic matter, dried (105 °C for 4 h), and weighed. The filters were recombusted at 450 °C for 4 h and weighed again to obtain inorganic suspended matter (ISM). By subtracting ISM from TSM, organic suspended matter was obtained.

In order to separate the dry weight of tripton from the dry weight of total particles, the dominant species of *Microcystis* and *Scenedesmus* in Lake Taihu were cultured in the laboratory to measure dry weight, Chl*a*, and P*a* concentrations in different growth periods. Surface algal-bloom samples were collected during calm-weather conditions and cleared using distilled water to obtain the relative pure phytoplankton (excluding tripton). Then, the sample was put under dark condition. Every three days, the sample was collected to measure the dry weight, Chl*a*, and P*a* concentrations. We found that a simple linear equation could describe the relation between the dry weight of phytoplankton and the sum of Chl*a* and P*a* concentrations

$$C_{\text{phytoplankton}} = 0.09 C_{\text{Chla+Pa}} (r^2 = 0.98, n = 31, p < 0.001) \quad (1)$$

where $C_{\text{phytoplankton}}$ is the dry weight of phytoplankton and $C_{\text{Chla+Pa}}$ is the sum of Chl*a* and P*a* concentrations. The concentration of tripton (C_{Tripton}) is obtained as the difference of TSM (C_{TSM}) and phytoplankton dry weight ($C_{\text{phytoplankton}}$).

C. Measurement of Remote-Sensing Reflectance and Inherent Optical Properties

Downwelling radiance and upwelling total radiance measurements were made by using an ASD field spectrometer (Analytical Devices, Inc., Boulder, CO) with a spectral response range of 350–1000 nm and a spectral resolution of 3 nm. The "above-water method" was used to measure water-surface spectra [16]. An optical fiber was positioned at nadir on a mount extending away from the boat to reduce the influence of reflectance off of the vessel on collected spectra. The radiance spectra from the reference panel, water, and sky were measured at a height of approximately 0.3 m above the water surface under clear-sky conditions. At each sampling site, the relevant spectra were measured ten times to optimize the signal-to-noise ratio and, thus, reduce the error of *in situ* measurements. Each spectrum was sampled 90° azimuthally from the Sun and

at a nadir viewing angle of 40°. The water-leaving radiance $L_{\mathrm{w}}(\lambda, 0^+)$ can be derived from the following:

$$L_{\mathrm{w}}(\lambda, 0^+) = L_{\mathrm{sw}}(\lambda, 0^+) - r_{\mathrm{sky}} \cdot L_{\mathrm{sky}}(\lambda) \tag{2}$$

where $L_{\mathrm{sw}}(\lambda, 0^+)$ is the upwelling radiance from the water and $L_{\mathrm{sky}}(\lambda)$ is the sky radiance measured at the same azimuth angle and at 40° zenith angle. The r_{sky} is the specular reflectance of skylight at the air–water interface ranging from 0.022 for calm weather to 0.025 for a wind speed of up to 5 $\mathrm{m} \cdot \mathrm{s}^{-1}$ [16]. A constant value of 0.0245 was used in this paper.

The incident downwelling irradiance $E_{\mathrm{d}}(\lambda, 0^+)$ was determined by measuring the radiance of the Lambertian reference panel $L_{\mathrm{p}}(\lambda, 0^+)$ as follows:

$$E_{\mathrm{d}}(\lambda, 0^+) = \pi L_{\mathrm{p}}(\lambda, 0^+)/\rho_{\mathrm{p}}(\lambda) \tag{3}$$

where $\rho_{\mathrm{p}}(\lambda)$ is the reflectance of the reference panel that has been accurately calibrated to 30%.

The remote-sensing reflectance above the water surface $R_{\mathrm{rs}}(\lambda, 0^+)$ is calculated as the ratio of water-leaving upwelling radiance $L_{\mathrm{w}}(\lambda, 0^+)$ to incident downwelling irradiance $E_{\mathrm{d}}(\lambda, 0^+)$. Some $R_{\mathrm{rs}}(\lambda, 0^+)$ spectra were excluded from the data set at sites with a thick algal bloom or macrophytes. A set of 176 $R_{\mathrm{rs}}(\lambda, 0^+)$ spectra was obtained in this paper.

The total absorption coefficient is the sum of the coefficients of tripton $[a_{\mathrm{d}}(\lambda)]$, phytoplankton $[a_{\mathrm{ph}}(\lambda)]$, CDOM $[a_{\mathrm{CDOM}}(\lambda)]$, and pure water $[a_{\mathrm{w}}(\lambda)]$

$$a(\lambda) = a_{\mathrm{d}}(\lambda) + a_{\mathrm{ph}}(\lambda) + a_{\mathrm{CDOM}}(\lambda) + a_{\mathrm{w}}(\lambda). \tag{4}$$

The absorption coefficient of pure water $a_{\mathrm{w}}(\lambda)$ reported by Smith and Baker [17] was used here. The coefficients $a_{\mathrm{p}}(\lambda)$ (the absorption coefficient of total particulate matter including tripton and phytoplankton), $a_{\mathrm{d}}(\lambda)$, and $a_{\mathrm{ph}}(\lambda)$ were determined by the quantitative filter technique [18], where methanol was used to partition the absorption of tripton and phytoplankton. Water samples were first filtered through a 47-mm-diameter Whatman fiberglass GF/F filter with 0.70-μm pores and, then, refiltered through a 25-mm-diameter Millipore filter with 0.22-μm pores to measure CDOM absorption. The measurement of the absorption coefficients of the three other components was undertaken using a Shimadzu UV-2401PC UV-Vis spectrophotometer; the detailed measurement process has been described by Zhang *et al.* [12]. The ratios of phytoplankton absorption to Chl*a* concentration and tripton absorption to tripton concentration are defined as the specific absorption coefficients of phytoplankton $a^*_{\mathrm{ph}}(\lambda)$ and tripton $a^*_{\mathrm{d}}(\lambda)$

$$a^*_{\mathrm{ph}}(\lambda) = a_{\mathrm{ph}}(\lambda)/C_{\mathrm{Chl}a} \tag{5}$$

$$a^*_{\mathrm{d}}(\lambda) = a_{\mathrm{d}}(\lambda)/C_{\mathrm{Tripton}} \tag{6}$$

where $C_{\mathrm{Chl}a}$ and C_{Tripton} are Chl*a* and tripton concentrations.

Beam attenuation of particulate matter except for pure water $c_{\mathrm{t-w}}(\lambda)$ was measured in a 4-cm path length cuvette against a reference of Milli-Q water between 350 and 800 nm at 1-nm intervals by a standard detector using a Shimadzu UV-2401PC UV-Vis spectrophotometer. The cuvette was positioned at a relatively large distance (5 cm) from the detector as described by Simis *et al.* [19]. The beam-attenuation coefficient was obtained based on the following [20]:

$$c_{\mathrm{t-w}}(\lambda) = 2.303 D(\lambda)/r \tag{7}$$

where $c_{\mathrm{t-w}}(\lambda)$ is beam-attenuation coefficient of particulate matter except for pure water at wavelength $\lambda(\mathrm{m}^{-1})$, $D(\lambda)$ is the optical density at wavelength λ, and r is the cuvette path length in meters. The factor of 2.303 was used to convert optical-density values from a base 10 log to a natural log scale.

$c_{\mathrm{t-w}}(\lambda)$ was expressed as the sum of the absorption and scattering coefficients of all particulate matter and CDOM. Because CDOM has no scattering, spectra of particle scattering $b_{\mathrm{p}}(\lambda)$ were obtained using the following:

$$b_{\mathrm{p}}(\lambda) = c_{\mathrm{t-w}}(\lambda) - a_{\mathrm{p}}(\lambda) - a_{\mathrm{CDOM}}(\lambda). \tag{8}$$

The backscattering coefficient $(b_{\mathrm{bp}}(\lambda))$ of the particles is calculated from the scattering coefficient of particles. The backscattering probability $(\beta = b_{\mathrm{bp}}/b_{\mathrm{p}})$ is dependent on the distribution of particles and on the refractive index. Sun *et al.* [21] found β ranged from 0.010 to 0.028 with a mean value of 0.018 ± 0.004 at 440 nm based on *in situ* measurement of absorption, beam attenuation, and scattering coefficients of 64 sites using AC-S and HS-6 in Lake Taihu in 2006. Although some studies showed that β can be weakly dependent on wavelength [22], [23]. However, Whitmire *et al.* [24] found that there was no significant spectral dependence of the spectral-backscattering probability β for each of five wavelengths in the range of 440–620 nm. Therefore, this paper took a mean β value of 0.018, as observed in Lake Taihu [21]. However, later on, we tested the impact of this assumption on the modeling and retrieval accuracy (in Section III-D).

The backscattering coefficient of pure water is half of the scattering coefficient. The scattering coefficient of pure water is adopted as follows [25]:

$$b_{\mathrm{bw}}(\lambda) = 0.5 b_{\mathrm{w}}(\lambda) = 0.00144 \left(\frac{\lambda}{500}\right)^{-4.32}. \tag{9}$$

The total backscattering coefficient was the sum of the backscattering coefficients of particles and pure water

$$b_{\mathrm{bt}}(\lambda) = b_{\mathrm{bp}}(\lambda) + b_{\mathrm{bw}}(\lambda). \tag{10}$$

D. Modeling of Remote-Sensing Reflectance

The remote-sensing reflectance just beneath the water surface $R_{\mathrm{rs}}(\lambda, 0^-)$ is calculated from irradiance reflectance $R(\lambda, 0^-)$, by dividing the latter by the so-called geometrical factor (Q), which is a wavelength-independent estimate of the ratio of the upwelling radiance $L_{\mathrm{u}}(\lambda, 0^-)$ to the downwelling irradiance $E_{\mathrm{d}}(\lambda, 0^-)$

$$R_{\mathrm{rs}}(\lambda, 0^-) = L_{\mathrm{u}}(\lambda, 0^-)/E_{\mathrm{d}}(\lambda, 0^-) = \frac{E_u(\lambda, 0^-)}{Q \cdot E_d(\lambda, 0^-)} = \frac{R(\lambda, 0^-)}{Q} = \frac{f}{Q} \cdot \frac{b_{\mathrm{bt}}(\lambda)}{a_{\mathrm{t}}(\lambda) + b_{\mathrm{bt}}(\lambda)}. \tag{11}$$

TABLE I
SEASONAL COMPARISON OF OPTICALLY ACTIVE SUBSTANCES AND OTHER INDEXES

		C_{TSM} mg l^{-1}	$C_{Tripton}$ mg l^{-1}	C_{Chla} μg l^{-1}	$a_{CDOM}(440)$ m^{-1}	Transparency cm	Depth m	T °C	V m s^{-1}
Winter (Jan.1–7)	Min	16.6	15.9	4.9	0.38	8	1.35	0.4	0.0
	Max	285.6	281.7	29.8	2.36	68	2.60	8.5	5.3
	Mean	130.2	128.2	16.5	0.98	17	2.04	3.7	2.57
	SD	57.8	57.7	6.6	0.33	9	0.34	2.2	1.45
Spring (Apr.25–27)	Min	15.9	14.4	4.9	0.35	10	1.60	17.1	0.00
	Max	213.9	129.0	448.9	1.52	60	2.80	23.0	5.90
	Mean	52.6	45.7	59.3	0.74	33	2.22	19.2	3.08
	SD	35.7	25.2	94.7	0.25	14	0.33	1.6	1.39
Summer (Jul.28–Aug.1)	Min	12.2	11.8	4.8	0.27	20	1.80	29.3	0.0
	Max	108.5	94.1	360.7	1.52	70	3.20	32.4	4.90
	Mean	48.4	43.2	50.6	0.71	34	2.47	31.1	3.12
	SD	23.2	19.4	58.1	0.26	12	0.36	1.0	0.97
Autumn (Oct.12–15)	Min	10.3	7.9	4.0	0.46	10	1.70	23.0	0.00
	Max	137.0	74.1	246.6	1.52	85	2.90	26.0	5.05
	Mean	31.3	26.0	35.7	0.84	38	2.37	24.3	2.63
	SD	21.0	12.8	46.9	0.20	12	0.30	0.8	1.15

T: water temperature: V: wind velocity; SD – standard deviation

The last term in (11) is the so-called Gordon approximation that relates the subsurface irradiance reflectance $R(\lambda, 0^-)$ to total absorption and scattering in an optically thick medium. Austin [26] proposed the factor of 0.544 for correlating radiance just above the surface to radiance just beneath the surface. Thus, remote-sensing reflectance just above the water surface $R_{\rm rs}(\lambda, 0^+)$ can be calculated as follows:

$$R_{\rm rs}(\lambda, 0^+) = 0.544 R_{\rm rs}(\lambda, 0^-) = 0.544 \frac{f}{Q} \cdot \frac{b_{\rm bt}(\lambda)}{a_{\rm t}(\lambda) + b_{\rm bt}(\lambda)}. \tag{12}$$

Monte Carlo studies [20] have found that f is mainly a function of solar-elevation angle that was reasonably well expressed as a linear function of μ_0, the mean cosine of the angles the photons make with the vertical just beneath the water surface

$$f = 0.975 - 0.629\mu_0. \tag{13}$$

The value of μ_0 is dependent upon the solar elevation and the proportion of direct and diffuse radiations. The value of μ_0 is calculated according to the sampling time, latitude, and solar-altitude angle.

Q in (11) was inversely related to μ_0. In theory, Q ranges from 0.3 to 6.5 but is generally expected to be 3–4 [27]. Here, an empirical equation of $Q = 2.38/\mu_0$ was used to calculate Q [6]. The mean values of f/Q in winter, spring, summer, and autumn were 0.158, 0.153, 0.152, and 0.157, respectively.

E. Data Analysis

The three sites with exquisitely high Chl*a* concentrations ($> 500\ \mu g \cdot L^{-1}$) were excluded from the data sets in this paper. Statistical analyses (mean value, linear and nonlinear fitting) were performed with the statistical package SPSS 11.0 for Windows. The root mean-square error (RMSE) and relative error (RE) of regression are calculated by the following:

$$\text{RMSE} = \sqrt{\frac{\sum_{i=1}^{n} (x_{\text{Est},i} - x_{\text{Obs},i})^2}{n}} \tag{14}$$

$$\text{RE} = \frac{(x_{\text{Est}} - x_{\text{Obs}})}{x_{\text{Obs}}} \times 100\% \tag{15}$$

where $x_{\text{Est},i}$ and $x_{\text{Obs},i}$ are the estimated and measured values, respectively, and n is the number of data points.

III. RESULTS AND DISCUSSION

A. Temporal and Spatial Variations in Optically Active Substances

There was a large variation in concentrations of the three optically active substances (TSM, Chl*a*, and CDOM) and other indexes (Table I), both within and between seasons, reflecting the temporal–spatial heterogeneousness of the large shallow lake.

The TSM concentration was significantly higher in winter than in other three seasons (ANOVA analysis, $p < 0.001$). In contrast, Chl*a* concentration was significantly lower in winter than in the other three seasons (ANOVA analysis, $p < 0.001$), corresponding to the absence and presence of marked algal blooms. Although there was no marked algal bloom in winter, Chl*a* concentration was still relatively high, with a mean value of $16.5 \pm 6.6\ \mu g \cdot L^{-1}$, demonstrating that Lake Taihu was a highly eutrophic lake. The mean values of TSM, tripton, and $a_{\rm CDOM}(440)$ in winter were 2.95, 3.35, and 1.29 times of those in other three seasons, respectively. However, the mean value of Chl*a* in winter was 0.34 times of that in other three seasons.

Some spatial differences were found for concentrations of optically active substances. Overall, the concentrations of the three optically active substances were higher in Meiliang Bay and the north of the lake than in the south. The mean

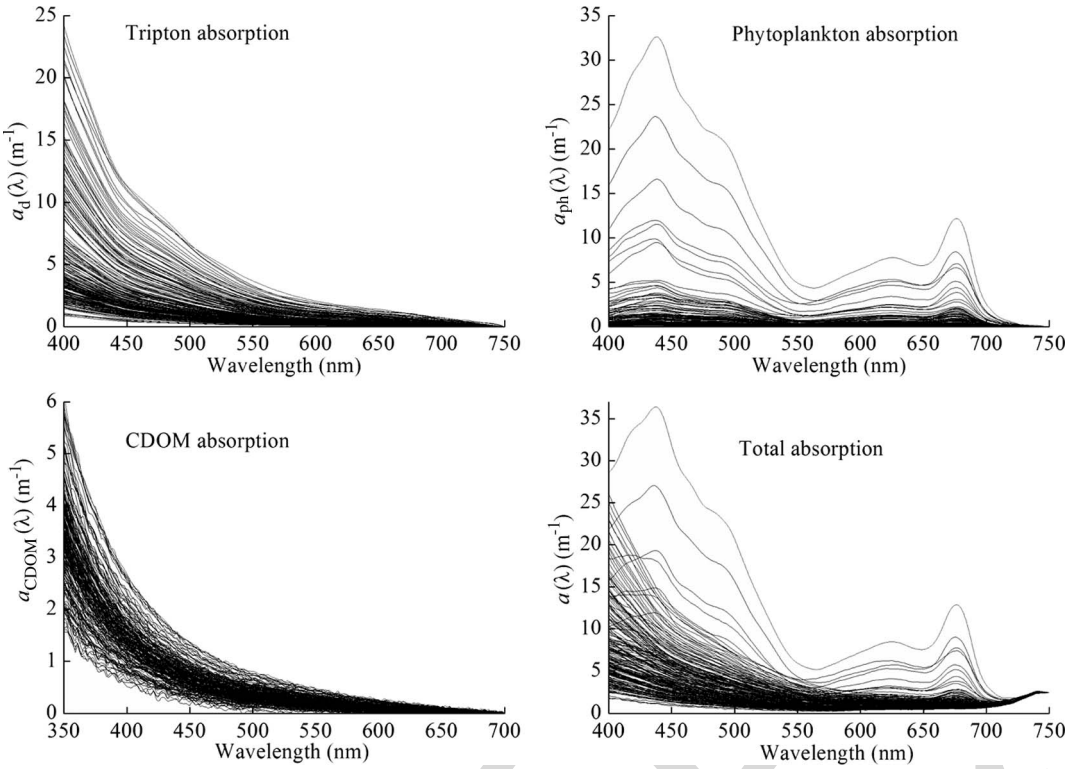

Fig. 2. Absorption spectra of tripton, phytoplankton, and CDOM and total absorption coefficients (lines represent different sites and cruises).

concentrations of Chl*a* and CDOM in transects 1, 2, and 3 were significantly higher than those in transect 4 (ANOVA analysis, $p < 0.001$) in all four seasons. However, the mean concentration of TSM did not differ significantly among the four transects in any season.

In summer and autumn, concentrations of TSM and Chl*a* were significantly higher in Meiliang Bay and the northern lake regions where serious algal blooms occurred. In contrast, in spring, the highest concentration of Chl*a* was in the southwest of the lake, near sites 39 and 40, where an intense algal bloom occurred.

In winter, the Chl*a* concentration remained at a relative low level for the whole lake as compared to other three seasons. In winter, the overall TSM concentrations were relatively high, due to deformation and disappearance of submerged aquatic vegetation and the marked sediment resuspension caused by the significant wind-induced wave action prior to the sampling dates. The mean wind velocity on January 4, 5, and 6 were 7.2, 5.6, and 6.6 m $\cdot$ s^{-1}, respectively, based on the automatic anemometer measurement of every 10 min in Taihu Lake Laboratory Ecosystem Research Station, which was located in the littoral of Lake Taihu.

In winter, there was no correlation between C_{TSM} and $C_{\mathrm{Chl}a}$; however, in the other three seasons, there was a significant positive correlation $(p < 0.001)$. This suggests that the interdependence between TSM and Chl*a* was quite strong in spring, summer, and autumn due to the frequent algal blooms which have a large contribution to TSM. TSM contained both organic and inorganic particles. For those with algal bloom, TSM contained a large amount organic matter in addition to the inorganic matter.

B. Variation in Absorption Coefficients

The spectral absorption coefficients of tripton, phytoplankton, CDOM, and the total absorption coefficient are shown in Fig. 2.

The absorption coefficient of CDOM approached zero near 700 nm and increased exponentially with decreasing wavelength over the 350–700-nm range. In previous studies, hyperbolic fitting has been suggested as a better approach than linear fitting [12], [28]. Thus, in this paper, hyperbolic fitting was used to fit CDOM spectra for wavelengths of 300–600 nm, considering that the CDOM absorption coefficient was near-zero or negative over a wavelength range larger than 600 nm. The mean and standard deviation of the spectral slope (S) for CDOM absorption were 6.36 and 0.83 nm^{-1}, respectively, based on the 197 data points (50 sites $\times$ 4 seasons $-$ 3 points with high Chl*a*). These values for the whole year were very close to the values for winter and summer [12]. Therefore, CDOM absorption can be expressed by

$$a_{\mathrm{CDOM}}(\lambda) = a_{\mathrm{CDOM}}(440)(\lambda/440)^{-6.36}. \tag{16}$$

The absorption coefficient of tripton decreased with increasing wavelength in all four seasons (Fig. 2). Many studies have shown that tripton has relatively stable absorption characteristics, which can be described using an exponential function [29], [30]. Considering that the absorption spectral shape of CDOM and tripton was very similar in this paper, a hyperbolic fit of the tripton absorption spectra was performed. Based on a large data set of 727 samples, collected from different regions of Lake Taihu from July 2004 to April 2007, it was found that the hyperbolic model was more accurate in its representation

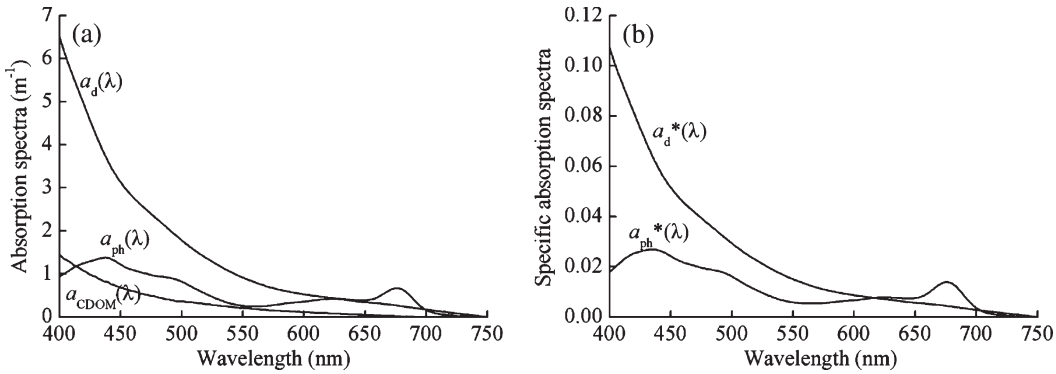

Fig. 3. (left) Mean absorption spectra of tripton ($a_{\rm d}(\lambda)$), phytoplankton ($a_{\rm ph}(\lambda)$), and CDOM ($a_{\rm CDOM}(\lambda)$) and (right) specific absorption coefficient spectra of tripton ($a^*_{\rm d}(\lambda)$) and phytoplankton ($a^*_{\rm ph}(\lambda)$) ($a^*_{\rm ph}(\lambda)$ unit: $\rm m^2 \cdot mg^{-1}$; $a^*_{\rm d}(\lambda)$: $\rm m^2 \cdot g^{-1}$).

of the tripton absorption than the simple exponential model (unpublished data). The range of spectral slope values ($S_{\rm d}$) for tripton in the wavelength range 400–700 nm in this paper, using hyperbolic fitting, was relatively narrow from 4.96 to 7.50 $\rm nm^{-1}$, with a mean value of 6.27 $\rm nm^{-1}$ and a coefficient of variation of 6.1%. The mean values of the spectral slopes of CDOM (6.36 $\rm nm^{-1}$) and tripton (6.27 $\rm nm^{-1}$) were very close. For all four seasons, tripton absorption can be expressed as follows:

$$a_{\rm d}(\lambda) = a_{\rm d}(440)(\lambda/440)^{-6.27}. \quad (17)$$

The absorption spectra of phytoplankton showed that the pigments had two diagnostic absorption peaks, in the blue wavelength (approximately 440 nm) and in the red wavelength (approximately 675 nm) (Fig. 2). However, the absorption coefficients of phytoplankton varied significantly in space and time because of marked differences in pigment concentrations. Phytoplankton absorption was very high at some sites during the algal blooms in spring, summer, and autumn.

Total absorption spectra were very similar to those of tripton, decreasing from 400 to 600 nm, except for several sites that had serious algal blooms on the water surface (Fig. 2), indicating the strong absorption by tripton in this shallow lake with its high tripton concentration (7.9–281.7 $\rm mg \cdot L^{-1}$). The mean absorption of tripton, phytoplankton, and CDOM also showed that tripton dominated the total absorption spectra [Fig. 3(a)]. Specific absorption spectra of phytoplankton in this paper fell within the range found in a range of water bodies [29], [31] but with a relatively low value as compared to the clear oceanic waters due to high Chl*a* concentration in Lake Taihu [Fig. 3(b)]. Specific absorption coefficient of phytoplankton has a tendency to decrease with increasing Chl*a* concentration due to the so-called package effect. The mean value of $a_{\rm d}(443)$ of 0.057 $\rm m^2 \cdot g^{-1}$ was higher than the one of 0.041 $\rm m^2 \cdot g^{-1}$ obtained by Babin *et al.* [31]. The difference can be partly attributed to the different calculation method. We note that Babin *et al.* [31] calculated specific absorption coefficient of tripton using TSM concentration (including phytoplankton). However, we calculated tripton concentration by excluding phytoplankton. This effect is expected to be the most important in eutrophic Lake Taihu where phytoplankton represents an important fraction of TSM during algal bloom in summer. Furthermore, the difference in the sources and mineral composition for coastal and lake waters may also cause the difference in $a^*_{\rm d}(443)$.

C. Modeling of Remote-Sensing Reflectance

For each station, the above-water remote-sensing reflectance was modeled according to (12) and (13). The total absorption and backscattering were taken from the measured inherent optical properties and application of (4), (8), (9), and (10).

The seasonal variation in remote-sensing reflectance is shown in Fig. 4. The large variability in the concentration of the three optically active substances and in their inherent optical properties resulted in large spatial and temporal variabilities in the magnitude of the modeled remote-sensing reflectance spectra. The reflectance spectra were highly variable at different sites and seasons. To validate the modeled $R_{\rm rs}(\lambda, 0^+)$, Fig. 5 shows the comparison of measured and modeled $R_{\rm rs}(\lambda, 0^+)$ at two typical sites in July 2006. There was a very good match of the measured and modeled $R_{\rm rs}(\lambda, 0^+)$, suggesting that it was reasonable and feasible to model remote-sensing reflectance based on the measurements of the beam-attenuation coefficient and the absorption coefficient in the laboratory. However, the $R_{\rm rs}(\lambda, 0^+)$ modeled was generally lower than the measured value at shorter wavelengths, less than 550 nm; this error being attributed to the uncertainty of scattering and backscattering coefficients. The scattering coefficient was calculated from beam-attenuation and absorption coefficients measurement made with a spectrophotometer (8), and since the spectrophotometer had an acceptance angle of 5°, some backscattered radiation was lost. Because the backscattering coefficient increased with decreasing wavelength, this loss term is greater at shorter wavelengths, causing the modeled $R_{\rm rs}(\lambda, 0^+)$ to be generally lower than the measured value. The difference in measured and modeled $R_{\rm rs}(\lambda, 0^+)$ could also have arisen from the errors in the observed $R_{\rm rs}(\lambda, 0^+)$. Although the water was placid in most cases, the potential for error due to skylight reflection still existed. Furthermore, the reflectance of air–water interface, which was slightly dependent on wind waves and set as a constant in this paper, induced a potential error.

These modeled spectra were very close in magnitude, shape, and spectral features to the typical reflectance spectra previously measured in Lake Taihu [14]. Remote-sensing reflectance

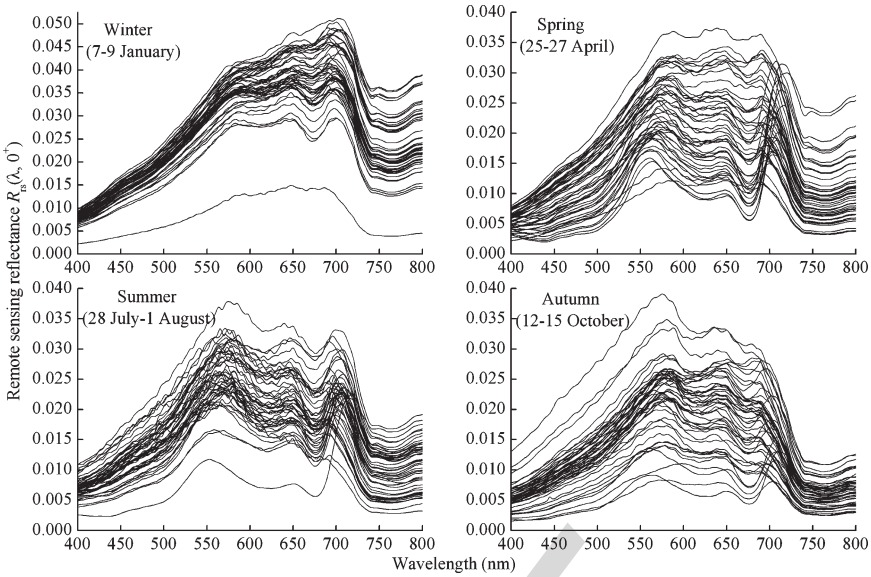

Fig. 4. Remote-sensing reflectance in four different seasons (lines represent different sites.)

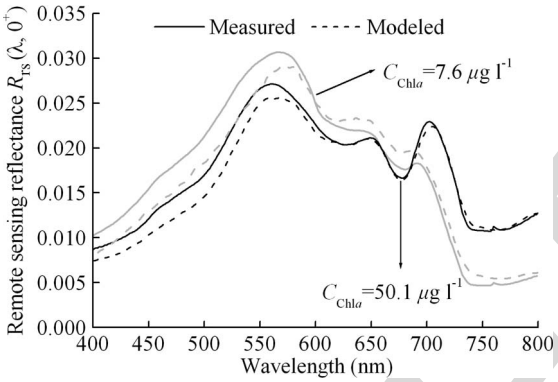

Fig. 5. Comparison of measured and modeled remote-sensing reflectance just above the water surface $R_{\mathrm{rs}}(\lambda, 0^+)$ from two sites in July 2006.

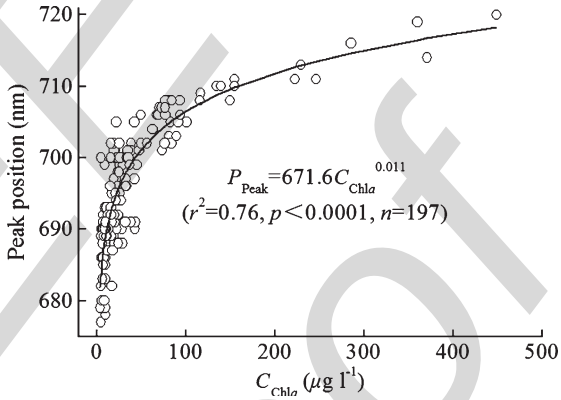

Fig. 6. Position of remote-sensing reflectance peak near 700 nm versus Chl*a* concentrations.

is proportional to the ratio of spectral backscattering to the sum of spectral absorption and backscattering of all optically active substances (12). Spectral reflectance peaks and local minima were generally inversely related to the total absorption spectra. In general, reflectance peaks occurred at around 560, 650, and 700 nm (Figs. 4 and 5). Reflectance minima occurred at short wavelengths near 400 nm due to strong absorption by particulate and dissolved substances (Fig. 2) and near 800 nm due to pure-water absorption. As the modeled reflectance spectra were calculated from the measured absorption and backscattering coefficients, the effect of bottom reflectance to the total reflectance was eliminated. However, the bottom reflectance might affect the *in situ* measured reflectance, particularly in the typical macrophyte-dominated regions (Xukou Bay and East Lake Taihu) [11]. For example, previous studies [13], [32] got the significant error of Chl*a* concentration and water quality in the two bays (Xukou Bay and East Lake Taihu) based on *in situ* measured and remotely derived $R_{\mathrm{rs}}(\lambda, 0^+)$.

In turbid Lake Taihu, absorption by dissolved organic matter and tripton and scattering by particulate matter contributed most to reflectance in the range of 400–500 nm, and a common characteristic of reflectance spectra in this range was low sensitivity to the variation of Chl*a* concentration. As a result, the blue-to-green ratio $R_{\mathrm{rs}}(440)/R_{\mathrm{rs}}(550)$ could not be used to estimate $C_{\mathrm{Chl}a}$ in waters studied. Therefore, the difference in measured and modeled $R_{\mathrm{rs}}(\lambda, 0^+)$ at short wavelengths had no effect on $C_{\mathrm{Chl}a}$ estimation in Lake Taihu. A peak in the green range near 550–570 nm (Figs. 4 and 5) was due to the minimal absorption of all algal pigments (Fig. 2), and scattering by ISM and phytoplankton cells controlled the magnitude of reflectance in this range. At around 675 nm, the reflectance minimum was due to phytoplankton absorption, particularly in sites with high pigment concentration. However, reflectance in this range was strongly affected by tripton concentration, in addition to Chl*a* concentration in turbid Lake Taihu, which decreased the correlation between $R_{\mathrm{rs}}(675)$ and $C_{\mathrm{Chl}a}$. A local minimum around 625 nm was due to phycocyanin absorption. This pigment is present primarily in cyanobacteria, and thus, a local reflectance minimum at 625 nm has often been used to monitor cyanobacterial blooms in eutrophic lakes [8], [9].

A marked peak was recorded near 700 nm, which corresponded to the decrease of particle scattering and the increase of pure-water absorption. The position of this peak shifted toward longer wavelengths with increasing Chl*a* concentration. Fig. 6 shows that peak position was closely related to $C_{\mathrm{Chl}a}$

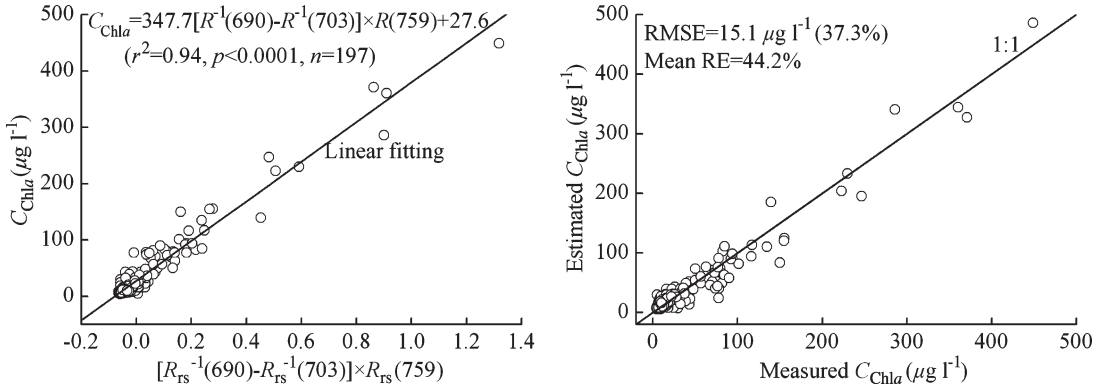

Fig. 7. Retrieval model of Chl*a* concentration and comparison of measured and estimated values using the three-band reflectance model (37.3% in the bracket is the percentage of RMSE accounting for the mean $C_{\mathrm{Chl}a}$).

concentration. This shows that, in addition to Chl*a* absorption, scattering by tripton played a significant role in controlling reflectance in this spectral region. The red-shifting of the reflectance peak position near 700 nm with increasing Chl*a* concentration was observed in other productive turbid waters [33], [34].

Our measurements in Lake Taihu were performed over a wide range of biooptical characteristics of water in different seasons at different solar zenith angles (ranging from 15° to 77°). However, the standard deviation of the f/Q values estimated was less than 2.5%, with a mean f/Q value of 0.1553, which was very close to the value reported in Case-1 waters [35]. Although both f and Q were largely dependent on solar zenith angle and the inherent optical properties of water, f/Q was basically independent of solar zenith angle. These results suggest that, for the nadir viewing the geometry of our measurements in these Case-2 waters, the observed variability in the quantity f/Q was not very large and not markedly different from Case-1 waters.

D. Retrieval Model of Chla

Obtaining accurate information on the temporal–spatial variation of Chl*a* concentration and algal blooms in Lake Taihu is critical for water-quality monitoring, understanding the mechanisms of eutrophication, and for issuing warnings to safeguard the drinking-water plants surrounding Lake Taihu. However, the application of currently operational satellite Chl*a* algorithms, such as MERIS, in the extremely turbid waters of Lake Taihu often results in erroneous retrievals.

In previous studies of Lake Taihu, single-band, band-ratio, and one-order derivative methods were used to estimate $C_{\mathrm{Chl}a}$ [13], [14]. In contrast, in this paper, a three-band reflectance model was used to estimate $C_{\mathrm{Chl}a}$ under conditions of high turbidity and high algal biomass. This model was tested on its accuracy and ability to perform for all seasons.

Recently, a conceptual model containing remote-sensing reflectance in three spectral bands in the red and near-infrared (NIR) range of the spectrum was suggested for retrieving Chl*a* in turbid productive waters [33], [34], [36]

$$\mathrm{Chl}a = A \times \left[R_{\mathrm{rs}}^{-1}(\lambda_1) - R_{\mathrm{rs}}^{-1}(\lambda)_2\right] \times R_{\mathrm{rs}}(\lambda_3) + B \quad (18)$$

where A and B are constants that are dependent on the specific inherent optical properties, and the three wavelengths have to be determined *a priori* or *a posteriori*.

The three-band reflectance model was originally developed for estimating pigment contents in terrestrial vegetation. Reciprocal reflectance in the first spectral band λ_1 should be most sensitive to $C_{\mathrm{Chl}a}$. $R_{\mathrm{rs}}(\lambda_1)$ is also affected by absorption by tripton, CDOM, and water as well as backscattering by all particulate matter. The effect of backscattering and the absorption by tripton and CDOM can be minimized using a second spectral band, where $R_{\mathrm{rs}}(\lambda_2)$ is minimally sensitive to absorptions by phytoplankton, tripton, and CDOM. $R_{\mathrm{rs}}(\lambda_3)$ is minimally affected by phytoplankton, tripton, and CDOM, and the total absorption the third band is a measure of the absorption by water. Based on these assumptions, the spectral ranges of three bands are restricted to 660–690, 700–750, and 730–750 nm, respectively. We refer to Dall'Olmo and Gitelson [36] and Gitelson *et al.* [34] for a detailed description and explanation of this choice of bands. Some studies showed that the three-spectral-band reflectance model $[R_{\mathrm{rs}}^{-1}(\lambda_1) - R_{\mathrm{rs}}^{-1}(\lambda_2)] \times R_{\mathrm{rs}}(\lambda_3)$ was more precise than the band-ratio method.

In order to find the best three bands by which to estimate Chl*a* concentration in Lake Taihu, the combinations of any three wavelengths of λ_1 from 660 to 690 nm, λ_2 from 700 to 750 nm, and λ_3 from 730 to 750 nm were used for correlation with $C_{\mathrm{Chl}a}$ using the remote-sensing reflectance modeled. The optimal band combination was judged by RMSE in this paper. Linear correlation showed that the three-band reflectance model $[R_{\mathrm{rs}}^{-1}(690) - R_{\mathrm{rs}}^{-1}(703)] \times R_{\mathrm{rs}}(759)$ gave the lowest RMSE, the highest correlation coefficient ($r^2 = 0.94$), and estimation precision. The resulting Chl*a* estimation model and the comparison of measured and estimated $C_{\mathrm{Chl}a}$ are shown in Fig. 7. The RMSE and the mean RE were 15.1 $\mu\mathrm{g} \cdot \mathrm{L}^{-1}$ (37.3% from the mean $C_{\mathrm{Chl}a}$) and 44.4%, respectively. Although $[R_{\mathrm{rs}}^{-1}(690) - R_{\mathrm{rs}}^{-1}(703)] \times R_{\mathrm{rs}}(759)$ gave the lowest RMSE, the corresponding RE was slightly larger than the lowest value of 42.5%. The measured and estimated values for $C_{\mathrm{Chl}a}$ were distributed along the 1:1 line, indicating that the three-band reflectance model $[R_{\mathrm{rs}}^{-1}(690) - R_{\mathrm{rs}}^{-1}(703)] \times R_{\mathrm{rs}}(759)$ could be used for the eutrophic turbid waters of Lake Taihu.

From (11) and (12), it can be concluded that the error sources for modeled remote-sensing reflectance are derived from the f/Q and the backscattering probability (β). However, for the

TABLE II
COMPARISON OF RETRIEVAL EQUATION OF THREE-BAND MODEL AND PRECISION FOR FIVE DIFFERENT VALUES OF THE BACKSCATTERING PROBABILITY (β)

β	Retrieval equation*	r^2	RMSE (m^{-1})	RE (%)
0.012	C_{Chla}=322.3x+27.6	0.94	15.4	45.1
0.015	C_{Chla}=335.1x+27.6	0.94	15.2	44.5
0.018	C_{Chla}=347.7x+27.6	0.94	15.1	44.2
0.021	C_{Chla}=360.2x+27.6	0.94	15.0	44.1
0.024	C_{Chla}=372.4x+27.6	0.94	15.0	44.1

*: Here x is $[R_{rs}^{-1}(690)\text{-}R_{rs}^{-1}(703)]\times R_{rs}(759)$

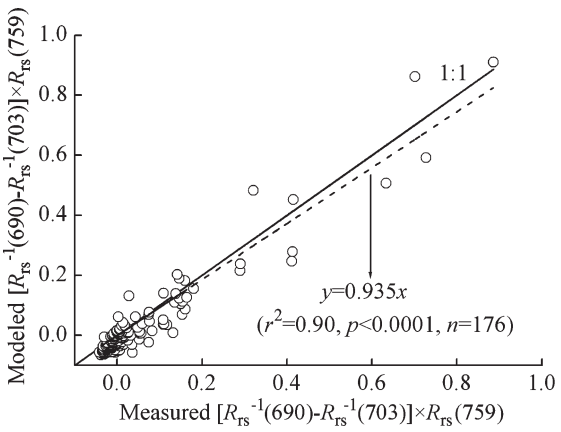

Fig. 8. Comparison of measured and modeled $[R_{rs}^{-1}(690) - R_{rs}^{-1}(703)] \times R_{rs}(759)$.

three-band model, f/Q is independent on the wavelength and will be eliminated in the model, thus has no effect on retrieval precision of C_{Chla}. In this paper, the values of 0.012, 0.015, 0.021, and 0.024 (33% standard deviation as compared to 0.018) were used to check the sensitivity of the three-band model to β for Chl*a* retrieval precision. Table II shows the fitting equation, r^2, RMSE, and RE of C_{Chla} estimation using the different β values. The variation of β only had a slight effect on the RMSE and RE of C_{Chla} precision. The maximal deviation of RMSE and RE were 1.9% and 2.1%, respectively, using 0.012 as β value as compared to the model using 0.018. Furthermore, the different β value only changed the linear slope but not the intercept of retrieval model. The results suggested that the three-band model developed in this paper was not sensitive to the uncertain parameters and could be used to C_{Chla} estimation.

Furthermore, Fig. 8 shows the comparison of measured and modeled $[R_{rs}^{-1}(690) - R_{rs}^{-1}(703)] \times R_{rs}(759)$ in order to further validate the three-band model using the remote-sensing reflectance modeled. Measured and modeled $[R_{rs}^{-1}(690) - R_{rs}^{-1}(703)] \times R_{rs}(759)$ were linked by a highly significant linear relationship ($r^2 = 0.90$), with a slope close to 1.0 (0.935) (Fig. 8). This analysis further showed that the modeled $R_{rs}(\lambda, 0^+)$ can be used to estimate C_{Chla} based on the three-band model as compared to measured $R_{rs}(\lambda, 0^+)$ spectra in other studies [33], [34], [36].

To compare the precision of the three-band reflectance model with other methods, the band-ratio method was also used to estimate C_{Chla}. To find the optimal spectral bands of the band-ratio method, the ratios of any two wavelengths from 350 to 800 nm were used for correlation with C_{Chla}. Linear correlation showed that the ratio of $R_{rs}(713)/R_{rs}(674)$ gave the highest determination coefficient ($r^2 = 0.92$) and the lowest RMSE (18.0 $\mu g \cdot L^{-1}$) (Fig. 9). The three-band reflectance model $[R_{rs}^{-1}(690) - R_{rs}^{-1}(703)] \times R_{rs}(759)$ was more precise than the band-ratio method $R_{rs}(713)/R_{rs}(674)$ as has been validated in other Case-2 waters [33], [34]. The three-band model with spectral bands optimized for inland waters, with Chl*a* ranging from 4.4 to 217.3 $\mu g \cdot L^{-1}$ [36] and from 107 to 3078 $\mu g \cdot L^{-1}$ [33], allowed accurate estimation of Chl*a* when applied to Lake Taihu, in spite of this lake having a very different composition of optically active substances (Chl*a*, tripton, and CDOM).

E. Retrieval Model Validation

In order to further understand the applicability of the three-band model, we presented the evaluation of the performance of the three-band model using an independent data set including two investigations. C_{Chla} ranged from 1.6 to 202.0 $\mu g \cdot L^{-1}$ with a mean value of 29.6 ± 36.6 $\mu g \cdot L^{-1}$, which fell into the range C_{Chla} used to develop the model. Comparisons of the measured and estimated C_{Chla} by the three-band model and the band-ratio model are shown in Fig. 10. Measured and estimated C_{Chla} by the three-band were in good agreement with a highly significant linear relationship ($r^2 = 0.92$ and a slope of 0.967 close to 1.0). The RMSE and percentage of RMSE accounting for the mean C_{Chla} of validation data set were lower than those of calibration data set (Figs. 7 and 10), suggesting that the performance of the three-band was accepted. Compared to the three-band model, the performance of the band-ratio method had a larger RMSE and RE (1.45 and 2.01 times of the three-band model, respectively). One of the reasons for the better performance of the three-band model, compared to the band-ratio method, was that the three-band model completely removed interferences due to backscattering by means of $R_{rs}(\lambda_2)$ and $R_{rs}(\lambda_3)$.

The three chosen bands basically fall into the range of MERIS channels (channels 8, 9, and 10: 681/8, 709/10, and 754/8 nm, respectively), which would make it possible to estimate Chl*a* accurately using MERIS imagery. The determination coefficient, RMSE, and the mean RE were 0.92, 17.0 $\mu g \cdot L^{-1}$, and 48.1%, respectively, using the central bands of MERIS imagery $[R_{rs}^{-1}(681) - R_{rs}^{-1}(709)] \times R_{rs}(754)$, which gave high retrieval accuracy.

Although the algorithms presented in this paper are derived for typical band settings of satelliteborne instruments like MERIS, it will still be quite challenging to investigate the applicability in actual MERIS or MODIS images of Lake Taihu. A major source of concern is the robustness of the algorithms for imperfect atmospheric correction over turbid waters [37], [38]. Small errors in the derivation of aerosol loading and the angstrom coefficient at near-IR wavelength typically translated in significant deviation for normalized water-leaving radiance at shorter wavelengths [39]. At present, the black-pixel assumption widely used in Case-1 waters for atmospheric correction was inappropriate in productive Case-2 waters with higher sediment or Chl*a* concentration. However, once the atmospheric correction procedures over extremely turbid waters have improved, the three-band algorithm might turn out to

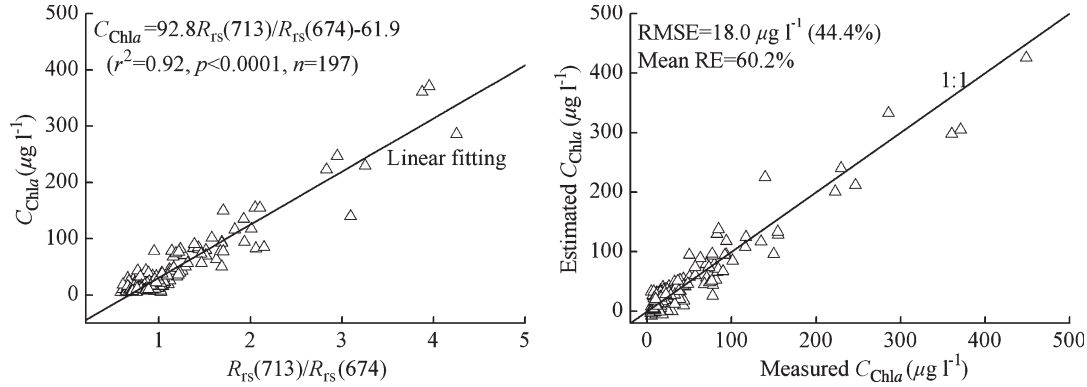

Fig. 9. Retrieval model of Chl*a* concentration and comparison of measured and estimated values using the band-ratio method (44.4% in the bracket is the percentage of RMSE accounting for the mean $C_{\mathrm{Chl}a}$).

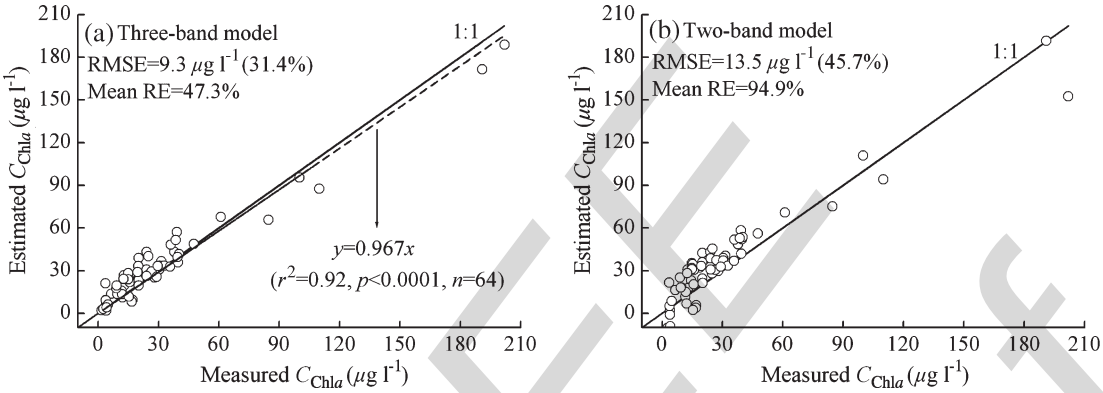

Fig. 10. Comparison of measured and estimated Chl*a* concentration ($C_{\mathrm{Chl}a}$) of the three-band model and band-ratio method based on an independent data set (31.4% and 45.7% in the bracket are the percentages of RMSE accounting for the mean $C_{\mathrm{Chl}a}$).

be a rather robust algorithm for Chl*a* retrieval, because the offsets in the $R_{\mathrm{rs}}(\lambda)$, due to errors in the atmospheric correction procedure, are partially counterbalanced by taking R_{rs} ratio's in a narrow wavelength interval (681–754 nm).

IV. Conclusion

Effective remote retrieval of Chl*a* is a major challenge in turbid and eutrophic Case-2 waters such as Lake Taihu in China. Although several previous studies have provided reliable detection of Chl*a* in Case-1 waters, many studies were not able to fully support accurate identification, monitoring, and forecasting of future locations of algal blooms in optically complex Case-2 waters. The retrieval accuracy of Chl*a* in Lake Taihu depends to a large extent on the accuracy of, and consistency among, the *in situ* data used in the development, validation, and improvement of the applied remote-sensing bio-optical algorithms. In this paper, biooptical measurements from four different seasons, with large temporal–spatial variability in the concentration of three optically active substances and inherent optical properties, were used to model the variation of remote-sensing reflectance. We found that the three-band model $[R_{\mathrm{rs}}^{-1}(690) - R_{\mathrm{rs}}^{-1}(703)] \times R_{\mathrm{rs}}(759)$ in the red and NIR wavelengths, where impact from CDOM and tripton absorptions on reflectance was minimal, could be used to retrieve Chl*a* with better performance than the band-ratio method widely used in previous studies. The wavelengths proposed for the three-band algorithm correspond well to the MERIS bands and provide a good basis for satellite monitoring of phytoplankton blooms in Case-2 waters from MERIS. It was noteworthy that the three-band model using MERIS central bands $[R_{\mathrm{rs}}^{-1}(681) - R_{\mathrm{rs}}^{-1}(709)] \times R_{\mathrm{rs}}(754)$ also allowed accurate estimation of Chl*a* in the range of Chl*a* from 4.0 to 448.9 $\mu\mathrm{g} \cdot \mathrm{L}^{-1}$ from four different seasons, suggesting that MERIS imagery could be used to monitor Chl*a* not only in waters with low-to-moderate Chl*a* concentrations (as has been done in previous studies) but also in extremely turbid and hypereutrophic waters. However, successful application of this algorithm to satellite data depends heavily on the accuracy of the atmospheric correction in the red–NIR region over lakes. This might pose new challenges to the positioning NIR bands in future missions and characterization of land influences on atmospheric correction over relatively small lakes like Lake Taihu.

Acknowledgment

The authors would like to thank S. Feng, X. Wang, Q. H. Zhao, and H. Zhang for their help with field-sample collection.

References

[1] B. Q. Qin, W. P. Hu, and W. M. Chen, *Process and Mechanism of Environment Changes of the Taihu Lake*. Beijing, China: Science Press, 2004, pp. 248–265. (in Chinese).

[2] L. Song, W. Chen, L. Peng, N. Wan, N. Gan, and X. Zhang, "Distribution and bioaccumulation of microcystins in water columns: A systematic investigation into the environmental fate and the risks associated with

microcystins in Meiliang Bay, Lake Taihu," *Water Res.*, vol. 41, no. 13, pp. 2853–2864, Jul. 2007.
[3] S. Z. Yu, "Drinking water and primary liver cancer," in *Primary Liver Cancer*. Beijing, China: Springer-Verlag, 1989, pp. 30–37.
[4] Y. Ueno, S. Nagata, T. Tsutsumi, A. Hasegawa, M. F. Watanabe, H. D. Park, G. C. Chen, G. Chen, and S. Z. Yu, "Detection of microcystins, a blue–green algal hepatotoxin, in drinking water sampled in Haimen and Fusui, endemic areas of primary liver cancer in China, by highly sensitive immunoassay," *Carcinogenesis*, vol. 17, no. 6, pp. 1317–1321, Jun. 1996.
[5] A. Dekker, T. Malthus, and E. Seyhan, "Quantitative modeling of inland water quality for high-resolution MSS-systems," *IEEE Trans. Geosci. Remote Sens.*, vol. 29, no. 1, pp. 89–95, Jan. 1991.
[6] H. J. Gons, "Optical teledetection of chlorophyll a in turbid inland waters," *Environ. Sci. Technol.*, vol. 33, no. 7, pp. 1127–1132, Apr. 1999.
[7] V. E. Brando and A. G. Dekker, "Satellite hyperspectral remote sensing for estimating estuarine and coastal water quality," *IEEE Trans. Geosci. Remote Sens.*, vol. 41, no. 6, pp. 1378–1387, Jun. 2003.
[8] S. G. H. Simis, S. W. M. Peters, and H. J. Gons, "Remote sensing of the cyanobacterial pigment phycocyanin in turbid water," *Limnol. Oceanogr.*, vol. 50, no. 1, pp. 237–245, Jan. 2005.
[9] T. Kutser, L. Metsamaa, N. Strömbeck, and E. Vahtmäe, "Monitoring cyanobacterial blooms by satellite remote sensing," *Estuar. Coast. Shelf Sci.*, vol. 67, no. 1/2, pp. 303–312, Mar. 2006.
[10] R. H. Ma, J. W. Tang, J. F. Dai, Y. L. Zhang, and Q. J. Song, "Absorption and scattering properties of water body in Lake Taihu, China: Absorption," *Int. J. Remote Sens.*, vol. 27, no. 19, pp. 4275–4302, Oct. 2006.
[11] B. Q. Qin, P. Z. Xu, Q. L. Wu, L. C. Luo, and Y. L. Zhang, "Environmental issues of Lake Taihu, China," *Hydrobiologia*, vol. 581, pp. 3–14, May 2007.
[12] Y. L. Zhang, B. Zhang, X. Wang, J. S. Li, S. Feng, Q. H. Zhao, M. L. Liu, and B. Q. Qin, "A study of absorption characteristics of chromophoric dissolved organic matter and particles in Lake Taihu, China," *Hydrobiologia*, vol. 592, pp. 105–120, Nov. 2007.
[13] R. H. Ma and J. F. Dai, "Investigation of chlorophyll-a and total suspended matter concentrations using Landsat ETM and field spectral measurement in Taihu Lake, China," *Int. J. Remote Sens.*, vol. 26, no. 13, pp. 2779–2787, Jul. 2005.
[14] H. B. Jiao, Y. Zha, J. Gao, Y. M. Li, Y. C. Wei, and J. Z. Huang, "Estimation of chlorophyll-a concentration in Lake Tai, China using in situ hyperspectral data," *Int. J. Remote Sens.*, vol. 27, no. 19, pp. 4267–4276, Oct. 2006.
[15] Y. L. Zhang, B. Q. Qin, and Z. J. Gong, "Spatial distribution of chromophoric dissolved organic matter fluorescence and its relation with absorption in Lake Taihu," *J. Agro-Environ. Sci.*, vol. 25, no. 5, pp. 1337–1342, Aug. 2006. [in Chinese with English abstract].
[16] J. W. Tang, G. L. Tiang, X. Y. Wang, X. M. Wang, and Q. J. Song, "The methods of water spectra measuring and analysis I: Above-water method," *J. Remote Sens.*, vol. 8, no. 1, pp. 37–44, Feb. 2004. [in Chinese with English abstract].
[17] R. C. Smith and K. S. Baker, "Optical properties of the clearest natural waters (200–800 nm)," *Appl. Opt.*, vol. 20, no. 2, pp. 177–184, 1981.
[18] B. G. Mitchell, "Algorithms for determining the absorption coefficient of aquatic particulates using the quantitative filter technique (QFT)," *Proc. SPIE*, vol. 1302, pp. 137–148, 1990.
[19] S. G. H. Simis, M. Tijdens, H. L. Hoogveld, and H. J. Gons, "Optical signatures of the filamentous cyanobacterium Leptolyngbya boryana during mass viral lysis," *Limnol. Oceanogr.*, vol. 52, no. 1, pp. 184–197, Jan. 2007.
[20] J. T. O. Kirk, *Light and Photosynthesis in Aquatic Ecosystem*. Cambridge, U.K.: Cambridge Univ. Press, 1994, pp. 1–431.
[21] D. R. Sun, Y. M. Li, C. F. Le, S. Q. Gong, H. J. Wang, L. Wu, and C. C. Huang, "Scattering characteristics of Taihu Lake and its relationship models with suspended particle concentration," *Environ. Sci.*, vol. 28, no. 12, pp. 2688–2694, Dec. 2007. [in Chinese with English abstract].
[22] C. D. Mobley, L. K. Sundman, and E. Boss, "Phase function effects on oceanic light fields," *Appl. Opt.*, vol. 41, no. 6, pp. 1035–1050, Feb. 2002.
[23] M. Tzortziou, J. R. Herman, C. L. Gallegos, P. J. Neale, A. Subramaniam, L. W. Harding, Jr., and Z. Ahmad, "Bio-optics of the Chesapeake Bay from measurements and radiative transfer closure," *Estuar. Coast. Shelf Sci.*, vol. 68, no. 1/2, pp. 348–362, Jun. 2006.
[24] A. L. Whitmire, E. Boss, T. J. Cowles, and W. S. Pegau, "Spectral variability of the particulate backscattering ratio," *Opt. Express*, vol. 15, no. 11, pp. 7019–7031, May 2007.
[25] A. Morel, "Optical properties of pure sea water," in *Optical Aspects of Oceanography*. London, U.K.: Academic, 1974, pp. 1–24.
[26] R. W. Austin, "Gulf of Mexico, ocean-colour surface-truth measurements," *Bound.-Layer Meteorol.*, vol. 18, no. 3, pp. 269–285, May 1980.
[27] A. Morel and B. Gentili, "Diffuse reflectance of oceanic waters. II. Bidirectional aspects," *Appl. Opt.*, vol. 32, no. 33, pp. 6864–6879, Nov. 1993.
[28] M. S. Twardowski, E. Boss, J. M. Sullivan, and P. L. Donaghay, "Modeling the spectral shape of absorption by chromophoric dissolved organic matter," *Mar. Chem.*, vol. 89, no. 1–4, pp. 69–88, Oct. 2004.
[29] A. Bricaud, A. Morel, M. Babin, K. Allali, and H. Claustre, "Variations of light absorption by suspended particles with chlorophyll a concentration in oceanic (case 1) waters: Analysis and implications for bio-optical models," *J. Geophys. Res.*, vol. 103, no. C13, pp. 31 033–31 044, Dec. 1998.
[30] C. S. Roesler, "Theoretical and experimental approaches to improve the accuracy of particulate absorption coefficients derived from the quantitative filter technique," *Limnol. Oceanogr.*, vol. 43, no. 7, pp. 1649–1660, Nov. 1998.
[31] M. Babin, D. Stramski, G. M. Ferrari, H. Claustre, A. Bricaud, G. Obolensky, and N. Hoepffner, "Variations in the light absorption coefficients of phytoplankton, nonalgal particles, and dissolved organic matter in coastal waters around Europe," *J. Geophys. Res.*, vol. 108, no. C7, pp. 1–20, Jul. 2003.
[32] X. J. Wang and T. Ma, "Application of remote sensing techniques in monitoring and assessing the water quality of Taihu Lake," *Bull. Environ. Contam. Toxicol.*, vol. 67, no. 6, pp. 863–870, Dec. 2001.
[33] P. V. Zimba and A. A. Gitelson, "Remote estimation of chlorophyll concentration in hyper-eutrophic aquatic systems: Model tuning and accuracy optimization," *Aquaculture*, vol. 256, no. 1–4, pp. 272–286, Jun. 2006.
[34] A. A. Gitelson, J. F. Schalles, and C. M. Hladik, "Remote chlorophyll-a retrieval in turbid, productive estuaries: Chesapeake Bay case study," *Remote Sens. Environ.*, vol. 109, no. 4, pp. 464–472, Aug. 2007.
[35] A. Morel and J. L. Mueller, "Normalized water-leaving radiance and remote sensing reflectance: Bidirectional reflectance and other factors," *Ocean Optics Protocols for Satellite Ocean Color Sensor Validation*, vol. 2, pp. 183–210, 2002. Rev3, NASA/TM-2002-210004.
[36] G. Dall'Olmo and A. A. Gitelson, "Effect of bio-optical parameter variability on the remote estimation of chlorophyll-a concentration in turbid productive waters: Experimental results," *Appl. Opt.*, vol. 44, no. 3, pp. 412–422, Jan. 2005.
[37] B. Bulgarelli and G. Zibordi, "Remote sensing of ocean colour: Accuracy assessment of an approximate atmospheric correction method," *Int. J. Remote Sens.*, vol. 24, no. 3, pp. 491–509, Feb. 2003.
[38] S. J. Lavender, M. H. Pinkerton, G. F. Moore, J. Aiken, and D. Blondeau-Patissier, "Modification to the atmospheric correction of SeaWiFS ocean colour images over turbid waters," *Cont. Shelf Res.*, vol. 25, no. 4, pp. 539–555, Mar. 2005.
[39] M. Darecki and D. Stramski, "An evaluation of MODIS and SeaWiFS bio-optical algorithms in the Baltic Sea," *Remote Sens. Environ.*, vol. 89, no. 3, pp. 326–350, Feb. 2004.

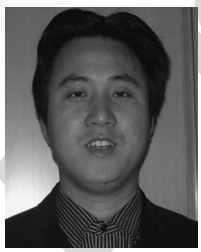

Yunlin Zhang received the B.S. degree in geography from Hunan Normal University, Changsha, China, in 1999 and the Ph.D. degree in physical geography from Nanjing Institute of Geography and Limnology, Chinese Academy of Sciences, Nanjing, China, in 2005.

Since 2005, he has been with Taihu Lake Laboratory Ecosystem Research Station, State Key Laboratory of Lake Science and Environment, Nanjing Institute of Geography and Limnology, Chinese Academy of Sciences, where he has been working in the general field of water optics and remote sensing of the environment. His main interests include lake optics, lake ecology, and the use of satellite data for lake water-quality monitoring.

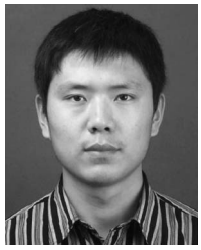

Mingliang Liu received the B.S. degree in environmental science from Nanjing Agricultural University in 2006. He is currently working toward the M.S. degree in geography in Taihu Lake Laboratory Ecosystem Research Station, State Key Laboratory of Lake Science and Environment, Nanjing Institute of Geography and Limnology, Chinese Academy of Sciences, Nanjing, China.

His main interests include the biooptical properties of and water-quality monitoring in shallow lake.

Boqiang Qin received the B.S. degree in hydrology from Hohai University, Nanjing, China, in 1984 and the Ph.D. degree in physical geography from Nanjing Institute of Geography and Limnology, Chinese Academy of Sciences, Nanjing, in 1993.

Since 1998, he has been a Professor of geophysics with Taihu Lake Laboratory Ecosystem Research Station, State Key Laboratory of Lake Science and Environment, Nanjing Institute of Geography and Limnology, Chinese Academy of Sciences. His research interests include hydrology, aquatic environmental sciences, and ecology.

Dr. Qin was a Guest Editor and has organized and published one Special Issue of *Hydrobiologia* and one supplement issue of *Sciences in China* in the last five years.

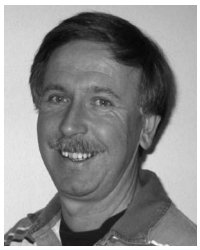

Hendrik Jan (Hans) van der Woerd received the Ph.D. degree in astrophysics from the University of Amsterdam, Amsterdam, The Netherlands, in 1987.

He was with the European Space Agency and the Dutch National Environmental Research Institute. Since 1997, he has been with the Institute for Environmental Studies, Vrije Universiteit, Amsterdam, where he has been working in the general field of remote sensing of the environment. His main interests include the validation and operational use of satellite data for water-quality monitoring in the coastal zone.

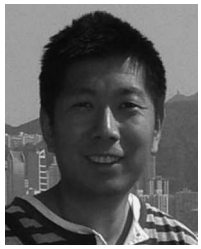

Junsheng Li received the B.S. degree in surveying and mapping from Tongji University, Shanghai, China, in 2002 and the Ph.D. degree from the Gradate School, Chinese Academy of Sciences, Beijing, China, in 2007.

In 2007, he was with the Institute of Remote Sensing Applications, Chinese Academy of Sciences. Since 2008, he has been with the Earth Observation and Digital Earth Science Center, Chinese Academy of Sciences. His research interests include environmental remote-sensing modeling and application and hyperspectral remote-sensing images processing.

Yunliang Li received the B.S. degree in geography from Hunan Normal University, Changsha, China, in 2006. She is currently working toward the M.S. degree in geographic information systems in Taihu Lake Laboratory Ecosystem Research Station, State Key Laboratory of Lake Science and Environment, Nanjing University, Nanjing, China.

Her major research interest includes remote-sensing mechanism and application.